ECS Transactions, 57 (1) 2885-2891 (2013)
10.1149/05701.2885ecst ©The Electrochemical Society

Fuel-flex SOFC Running on Internal Gradual Reforming

S. D. Nobrega[a,d], F. C. Fonseca[a], P. Gelin[b], F. B. Noronha[c], S. Georges[d], and M. C. Steil[d]

[a] Instituto de Pesquisas Energéticas e Nucleares, IPEN, São Paulo, SP, 05508-000, Brazil
[b] Institut de recherches sur la catalyse et l'environnement de Lyon, UMR 5256 CNRS-Université de Lyon 1, 69626 Lyon, France
[c] Instituto Nacional de Tecnologia, INT, Rio de Janeiro, RJ, 20081-312, Brazil
[d] Laboratoire d'Electrochimie et de Physicochimie des Matériaux et des Interfaces, UMR 5279, CNRS-Université de Grenoble, 38400 Saint Martin d'Hères, France

Electrolyte-supported single fuel cells based on yttria-stabilized zirconia components with a ceria-based catalytic layer added to the anode were operated with three different fuels: hydrogen, methane, and ethanol. Methane and ethanol were directly fed to the fuel cells without water or any oxidizing agent. Fuels were interchanged during continuous polarization and fuel cell accumulated ~160 hours of operation delivering comparable current densities for each fuel. This result was supported by stability curves, impedance spectroscopy, and energy-dispersive X-ray spectroscopy analyses, which showed that deleterious carbon deposits were absent in the anode of tested fuel cells.

Introduction

Fuel cell development is driven by the urgent need of high efficiency and less environmental impact for the increasing demand of energy. Solid oxide fuel cells (SOFCs) are potentially the most efficient technology to convert chemical energy into electricity and thus could have a major impact on reducing fuel consumption and CO_2 emissions (1,2). The high operating temperatures, typically $\geq$ 600°C, confer SOFCs the potential to run on both conventional fuels (e.g., natural gas, gasoline, and diesel) and biofuels (e.g., biogas, ethanol, and biodiesel). Such unique fuel flexibility, associated with high-efficiency, low (or zero) emissions, and unsolved problems concerning both the production and the storage of hydrogen, have encouraged a great number of studies on SOFCs operating with alternative fuels (3-7). However, several practical issues have prevented a more widespread use of fuels other than hydrogen. The catastrophic degradation of the standard Ni-based cermet anodes when carbon containing fuels are fed to the fuel cell is a major hurdle. Thus, effective demonstrations of fuel flexible SOFCs showing long term operation using different fuels with performance comparable to hydrogen are rarely found.

One of the most studied alternative fuel is methane because it is abundant and the main constituent of both natural and biogas; nonetheless, most of the reported alternative fuels for SOFCs have been non-renewable (3,8). One of the few notable exceptions is bioethanol (6,9). Sugarcane derived ethanol is a cost competitive and efficient biofuel that has received increasing attention (6,10,11). Ethanol is a liquid fuel that has high energy density that can be easily stored and transported, and has great potential for hydrogen production with high efficiencies and zero net carbon emission (10). As

compared to other renewables such as biodiesel and biogas, ethanol exhibits two important characteristics for SOFCs, fixed composition and insignificant sulphur contamination. In this context, the development of fuel-flexible anodes could disconnect SOFCs from the (still to come) hydrogen infrastructure and would greatly push this technology towards commercialization. Indeed, SOFC operation on biofuels is the most energy efficient means to utilize home grown carbon neutral fuels (2,10).

An interesting approach has been the decoupling of the catalytic and electrochemical functions of the anode by adding an active layer able to process the fuel and to protect the anode (12-14). By using such a catalytic layer some studies have demonstrated SOFCs running on carbon containing fuels with satisfactory performance and stability; however, most of those studies add water to the fuel to ensure the stability of the anode (15,16). Otherwise, the gradual internal reforming (GIR) was theoretically and experimentally demonstrated to result in long-term stability of SOFCs operating without added water (12-14,17), as shown in the schematic of Fig. 1.

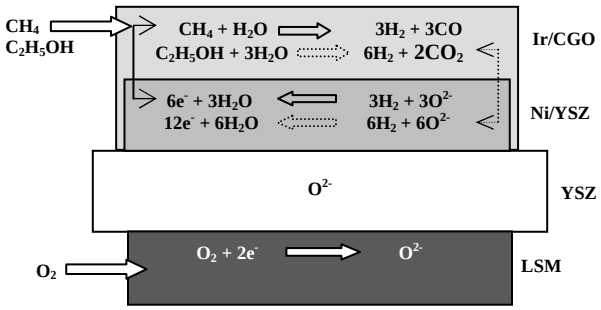

Figure 1. Scheme of gradual internal reforming unit cell and reactions on direct methane and ethanol. The unit cell is comprised of a lanthanum manganite (LSM) cathode, YSZ (yttria-stabilized zirconia) electrolyte, Ni/YSZ anode, and Ir/CGO (gadolinia-doped ceria) catalytic layer.

Thus, provided that an adequate catalyst is available, the GIR opens up the way for the development of fuel-flexible SOFCs. In the present study, an iridium/ceria-gadolinia (Ir/CGO) catalyst was used as the active layer in a SOFC operating in the gradual internal reforming with methane and ethanol.

Experimental

Fabrication and Characterization of Ir/CGO Catalyst

The catalytic layer of $Ce_{0.9}Gd_{0.1}O_{2-x}$ (CGO, Praxair) containing 0.1% mol of Ir (Ir/CGO) was prepared by an impregnation technique (18). The appropriate amount of iridium acetylacetonate (Alfa Aesar) solution in toluene was added to a suspension of CGO. After evaporation of the solvent under reduced pressure, the catalyst was calcined in flowing O_2 at 350°C for 6 h.

Fabrication and Tests of Solid Oxide Fuel Cells

Electrolyte supported cells were fabricated using substrates (56 mm diameter and ~1 mm thick) of yttria-stabilized zirconia (YSZ - 8 mol% yttria, Tosoh) produced by

uniaxial and isostatic pressing (2500 bar) followed by sintering at 1450°C for 2 h. Electrode layers with 13.8 cm^2 active area were deposited by spin coating: (a) $La_{0.65}Sr_{0.30}MnO_3$ (LSM) and LSM/YSZ (50/50 wt.%) for current collector and functional cathode layers, respectively; (b) Ni/YSZ 60/40 vol.% and 40/60 vol.% for current collector and functional anode layers, respectively; and (c) $Ir/Ce_{0.9}Gd_{0.1}O_{2-x}$ catalytic layer.

The Ir/CGO catalytic layer was deposited onto the anode by spray-coating of ethanol-based suspension with organic additives, and heat treated at 900°C for 2 h in flowing argon. The Fig. 2 shows the schematic diagram of electrolyte-supported single cell, with the arrangement of the fuel cell testing apparatus. The single cell was set up between two alumina tubes (anode and cathode side) using gold rings for the sealing.

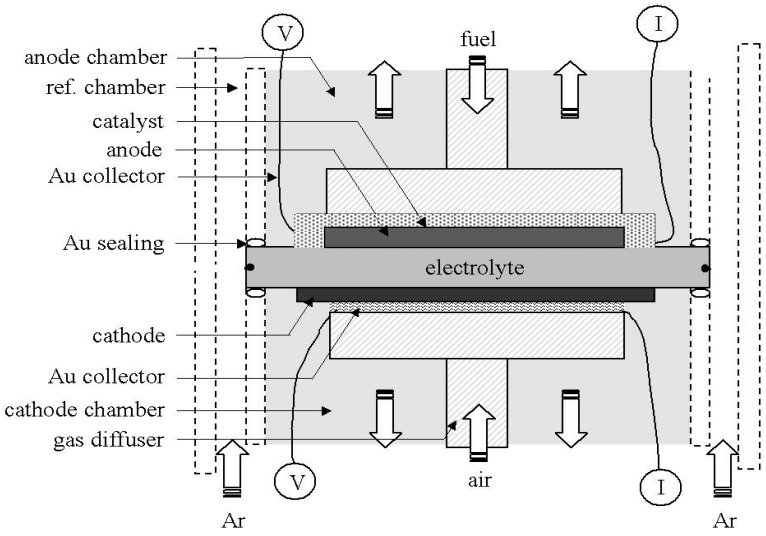

Figure 2. Schematic representation of the experimental setup used for single cell testing (13).

Alumina capillaries were inserted in the concentric tubes for both gas delivery and electric terminals. Gold wires allow independent measurements of the current and the potential in a 4-wire configuration. The system is closed with a metallic head sealed with rubber gaskets. Fuel cell tests were performed at 850°C with flowing synthetic air in the cathode side (5 L h^{-1}). Fuel cells were initially operated on H_2 (60%) and after anode reduction and stable OCV = 1.22 V, the electrochemical properties were studied under hydrogen, ethanol, and methane, without water addition. Hydrogen (60%) was switched to the desired fuel: methane (20%) or ethanol (10%). Fuels were carried by argon at total flow rate of 4 L h^{-1} set by calibrated mass flowmeters (Brooks Instr.). Liquid ethanol was kept in a thermal bath with controlled temperature of 29°C. Methane (Air Liquide, pure 99,94%). The fuel cell was continuously operated for ~160 hours during which the three studied fuels were repeatedly changed. Electrochemical impedance spectroscopy (EIS) and polarization vs. time (i-*t*) measurements were performed by an Autolab PGSTAT128N potentiostat with a BSTR10A current booster. A variable resistor bench connected in series with the fuel cell was used for polarization curve (V-i) measurements.

Scanning electron microscopy analyses of the fractured surface of the anode were carried out after the fuel cell operation.

Results and Discussion

The electrochemical properties of fuel cells operating on H_2/Ar (60/40%), CH_4/Ar (20/90%), and C_2H_5OH/Ar (10/90%) were studied. The Fig. 3 shows the time (*t*) dependence of *i* (at 0.6 V) using H_2, methane, and ethanol. The operation was initiated in H_2, and after a steady operation (~3 h), the fuel was switched to methane for ~10 h. After the operation with methane, the fuel was switched to hydrogen (~2 h) and then to ethanol for ~100 h, followed by H_2 (~40 h), summing up a total of ~160 h of continuous operation.

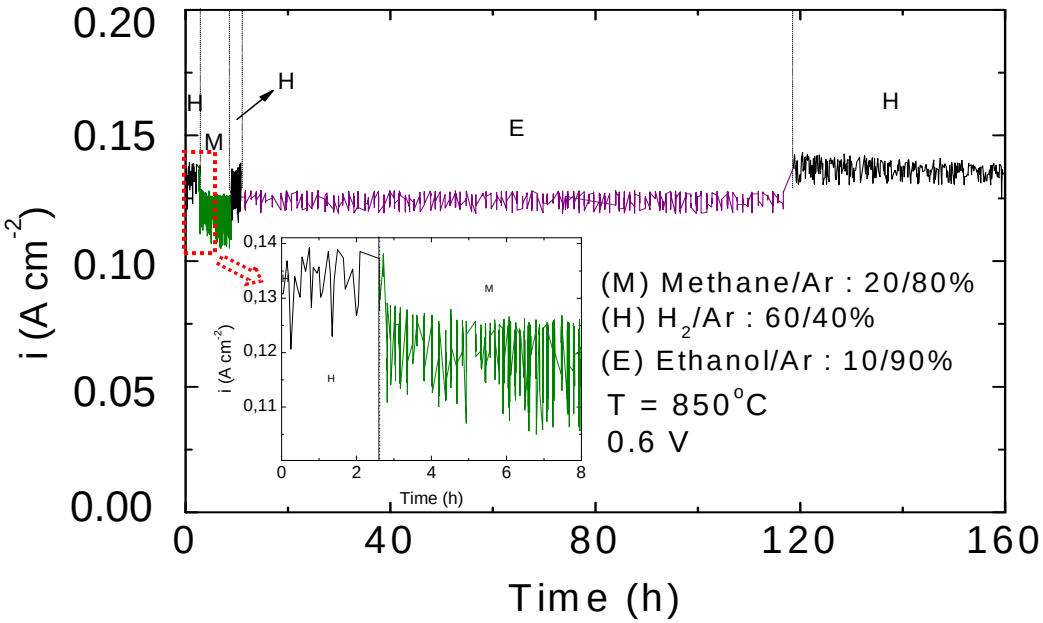

Figure 3. Potentiostatic test recorded at 0.6 V of a single SOFC containing a ceria-based catalytic layer under hydrogen, ethanol, and methane.

The most important result shown in Fig. 3 is the good stability of the fuel cell operating on three distinct fuels without water addition for a long time period. After initial operation on H_2 (~3 h), the fuel cell quickly stabilized under methane, with *i* ~0.12 A cm^{-2}. After ~10 h on methane, the fuel was changed to H_2, and after ~2 h of the stability, was switched to ethanol, in which a stable *i* ~0.125 A cm^{-2} was recorded for ~100 h. Finally, the ethanol was changed to hydrogen and once again and a rather stable *i* ~0.135 A cm^{-2} was measured for more than 40 hours. The current density at 0.6 V exhibited a total decay of ~3% in ~160 h of operation. This is a relatively high degradation rate when compared to the state-of-the-art fuel cells, but it is markedly lower than degradation resulting from carbon formation. The results shown in Fig. 3 are a strong indication that the catalytic layer protects the anode and prevents carbon deposition, which would result in fast and pronounced degradation of the fuel cell.

To further understand the operation of the fuel-flexible SOFCs and possible degradation mechanisms both impedance measurements and microstructural analyses were carried out. Figure 4 shows impedance data taken during the stability tests at polarization.

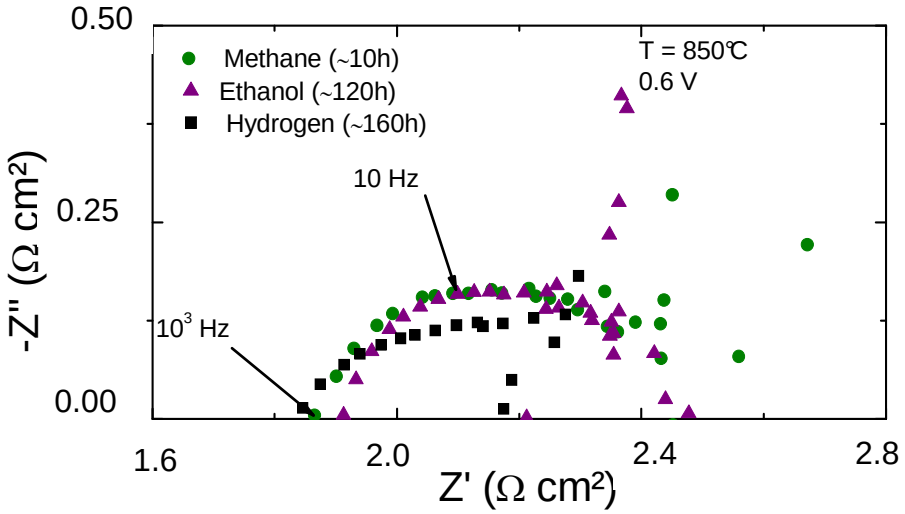

Figure 4. Impedance measurements at 0.6 V for the fuel cell operating in hydrogen, ethanol, and methane taken during the stability tests.

Fig. 4 shows impedance data under 0.6 V polarization collected for methane, ethanol and hydrogen at t ~ 10, 120, and 160 h, respectively. The impedance diagrams consist of a depressed semicircle arc, and the polarization resistance reflected the observed variation of i for each fuel (Fig. 4). As compared to hydrogen, both methane and ethanol exhibited slightly increased total resistance. The relatively similar impedance diagrams indicate that the anode reactions are comparable under different fuels, i.e., the hydrogen oxidation occurring at the Ni/YSZ layer, in agreement with the GIR mechanism.

To investigate possible degradation due to carbon deposition on the anode, the fuel cell was analyzed by EDX. The spectrum of the EDX is shown in the Fig. 5. The EDX spectrum exhibits the expected peaks corresponding to Zr, Y, Ni, O, and a minor contribution corresponding to carbon could be identified. Apparently, such minor carbon formation corresponds to non-graphitic carbon as indicated in the catalytic tests. Such carbon species are easily oxidized and in principle represent no major harm to the GIR (13,14).

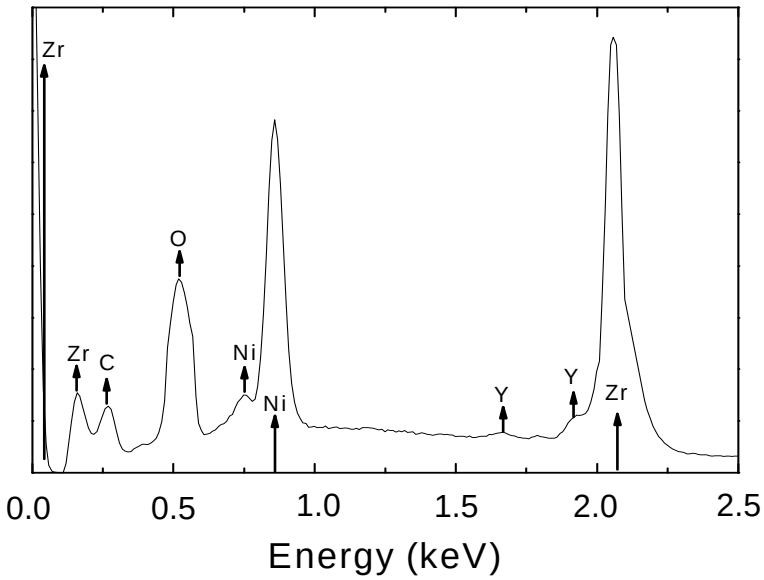

Figure 5. Energy dispersive X-ray spectroscopy of the anode after 160 h.

Conclusions

A fuel-flexible solid oxide fuel cell was demonstrated to operate on methane, bioethanol, and hydrogen for 160 hours. Stable current outputs in different fuels indicated that the gradual internal reforming was effective, preventing deleterious carbon formation and delivering similar current outputs under different fuels. Based on the present results, the design of both optimized fuel cells and catalyst open the way to the development of high-performance fuel-flexible SOFCs running directly on renewable fuels.

Acknowledgments

Thanks are due to the Brazilian agencies CAPES/COFECUB (698/2010), CNPq (304128/2010-4), CNEN, and FAPESP (2013/11914-3).

References

1. S.C. Singhal and K. Kendall, *High Temperature and Solid Oxide Fuel Cells – Fundamentals, Design and Applications*, p. 1-22 (2003).
2. E.D. Wachsman, C.A. Marlowe and K.T. Lee, *Energy Environ. Sci.*, **5**, 5498 (2007).
3. A. Atkinson, S. Barnett, R.J. Gorte, J.T.S. Irvine, A.J. Mcevoy, M. Mogensen, S.C. Singhal and J. Vohs, *Nat. Mater.*, **3**, 17 (2004).
4. Z. Zhan and S.A. Barnett, *Science*, **308**, 844 (2005).
5. S. Park, J.M. Vohs and R.J. Gorte, *Nature*, **404**, 265 (2000).
6. E.N. Armstrong, J. Park and N.Q. Minh, *Electrochem. Solid State Lett.*, **15**, B75 (2012).
7. J. Liu and S.A. Barnett, *Solid State Ionics*, **158**, 11 (2003).
8. S. Park, J.M. Vohs and R.J. Gorte, *Nature*, **404**, 265 (2000).
9. R. Muccillo, E.N.S. Muccillo, F.C. Fonseca and D.Z. de Florio, *J. Electrochem. Soc.*, **155**, B232 (2008).
10. G.A. Deluga, J.R. Salge and X.E. Verykios, *Science*, **303**, 993 (2004).
11. S.L. Douvartzides, F.A. Coutelieris, A.K. Demin and P.E. Tsiakaras, *Int. J. Hydrog. Energy*, **29**, 375 (2004).
12. P. Vernoux, J. Guindet and M. Kleitz, *J. Electrochem. Soc.*, **145**, 3487 (1998).
13. J.M. Klein, M. Hénault, P. Gélin, Y. Bultel and S. Georges, *Electrochem. Solid State Lett.*, **11**, B144 (2008).
14. J.M. Klein, M. Hénault, C. Roux, Y. Bultel and S. Georges, *J. Power Sources*, **193**, 331 (2009).
15. X.F. Ye, S.R. Wang, Z.R. Wang, L. Xiong, X.F. Sun and T.L. Wen, *J. Power Sources*, **177**, 419 (2008).
16. X.F. Ye, S.R., Wang, Q. Hu, Z.R. Wang, T.L. Wen and Z.Y. Wen, *Electrochem. Commun.*, **11**, 823 (2009).
17. S.D. Nobrega, M.V. Galesco, K. Girona, D.Z. De Florio, M.C. Steil, S. Georges and F.C. Fonseca, *J. Power Sources*, **213**, 156 (2012).
18. M. Wisniewski, A. Boréave and P. Gélin, *Catal. Commun.*, **6**, 596 (2005).
19. F.C. Fonseca and R. Muccillo, *Physica C*, **267**, 87 (1996).

20. V. Esposito, D. Z. de Florio, F. C. Fonseca, E. N. S. Muccillo, R. Muccillo and E. Traversa, *J. Eur. Ceram. Soc.*, **25**, 2637 (2005).
21. B. Huang, X. Zhu, W. Hu, Y. Wang and Q. Yu, *J. Power Sources*, **195**, 3053 (2010).
22. F.X. Ye, S.R. Wang, Q. Hu, J.Y. Chen, T.L. Wen and Z.Y. Wen, *Solid State Ionics*, **180**, 276 (2009).
23. E.P. Murray, T. Tsai and S.A. Barnett, *Solid State Ionics*, **110**, 235 (1998).
24. A. S. Ferlauto, D. Z. de Florio, F. C. Fonseca, V. Esposito, E. Traversa, R. Muccillo, L. O. Ladeira, *Catalysts Applied Physics A, Materials Science & Processing*, **84**, 271 (2006).